A MEASUREMENT OF SOLAR REFLECTIVITY OF BUILDING MATERIALS, TUCSON, ARIZONA

by

David Mark Acklam

A Thesis Submitted to the Faculty of the

DEPARTMENT OF ELECTRICAL ENGINEERING

In Partial Fulfillment of the Requirements
For the Degree of

MASTER OF SCIENCE

In the Graduate College

THE UNIVERSITY OF ARIZONA

1 9 7 7

STATEMENT BY AUTHOR

This thesis has been submitted in partial fulfillment of requirements for an advanced degree at The University of Arizona and is deposited in the University Library to be made available to borrowers under rules of the Library.

Brief quotations from this thesis are allowable without special permission, provided that accurate acknowledgment of source is made. Requests for permission for extended quotation from or reproduction of this manuscript in whole or in part may be granted by the head of the major department or the Dean of the Graduate College when in his judgment the proposed use of the material is in the interests of scholarship. In all other instances, however, permission must be obtained from the author.

SIGNED: David M Ashlem

APPROVAL BY THESIS DIRECTOR

This thesis has been approved on the date shown below:

John A. Reagan — 12-1-77

JOHN A. REAGAN — Date

Professor of Electrical Engineering

ACKNOWLEDGMENTS

I wish to thank Mr. Dale Byrne and Capt. Jay Huttenhow, USAF, for their assistance in the preparation of this thesis. I wish to express my appreciation for the cooperation and assistance given by: Beauty Built Homes, Corbett Roofing Co., Chastain Builders Inc., Estes Homes, Wood Bros. Homes, and the Phoenix Brickyard of Tucson. I also wish to thank the many homeowners and merchants that allowed me to use their properties to make these reflectance measurements. Last, I want to thank my wife for her patience and help in the making of these measurements and in the preparation of this thesis.

TABLE OF CONTENTS

LIST OF TABLES

LIST OF ILLUSTRATIONS

ABSTRACT

The measurement of solar reflectance values associated with building materials used in the Tucson, Arizona community is presented. The reflectance values, measured under actual solar exposures, were made using a hemispherical solar radiometer. A theoretical development of the total reflectance value is given. The concept of using a sensing element with a Lambertian response to measure this value is examined. A description is given of the instrumentation employed and of the experimentation conducted to verify that this instrumentation adequately measures the total reflectance. Details of the procedures used in measuring vertical, sloped, and horizontal surfaces are presented along with the limitations imposed by these types of measurements. The results of the measurements, from a sampling of the exterior surfaces used in this community, are cataloged. Results are also given of a comparison of measured versus published data pertaining to the diffuse solar radiation factor and the solar heat gain factor.

INTRODUCTION

Tucson, Arizona is representative of many of the architectures common to the Southwest. The measurement of solar reflectance values, from a sampling of exterior surfaces within this community, resulted in a catalog of data which are applicable throughout the Southwest. These data are of concern in the cooling load calculation because the solar radiation gains through the sunlit roof and exterior walls of a building are affected by the amount of radiant flux absorbed by these surfaces.

In addition to measuring reflectance values, the field measurements yielded solar data that were found to be comparable to interpolated data tabulated in the ASHRAE Handbook of Fundamentals (1972). Comparisons were made for data pertaining to the diffuse solar radiation factor and the solar heat gain factor.

Due to the large variety of building materials and methods of construction employed, a standardization of data documentation was necessary. Using brand names, for the purpose of identification only, along with general construction terminology, it was felt that there would be little doubt as to what the actual surface that was measured was. This type of standardization was realized with the assistance of several local home builders,

contractors, and merchants. The data were documented in order to follow, but not strictly adhere to, the ASHRAE Standard 74-73 (1973). This could not be achieved due to the type of instrumentation employed. The standard mandated a thermopile type pyreliometer, whereas, this study used a color compensated silicon cell type radiometer. The radiometer was capable of sensing the total radiant flux within the 0.45 μm to 0.95 μm bandwidth.

THEORETICAL DEVELOPMENT

Total Reflectance

The reflectance that we are interested in is that as described by Wolfe (1965, p. 25) called total reflectance. It is defined in general as the ratio of the total radiant power (in all directions) reflected to the total radiant power (in all directions) incident on a surface element. Looking at the geometry of the problem, Figure 1, we can describe the monochromatic differential power dP_i incident on a differential surface element dA_o at the origin due to radiation within a differential solid angle $d\Omega_i$ as

$$dP_i = L_s(\theta_i,\Phi_i,\lambda_i)dA_o d\Omega_i, \tag{1}$$

where $L_s(\theta_i,\Phi_i,\lambda_i)$ is the incident radiance and $d\Omega_i$ is given by

$$d\Omega_i = \mathrm{Sin}\theta_i d\theta_i d\Phi_i. \tag{2}$$

The total power incident on the surface element is given by

$$P_i = \int_{\lambda_1}^{\lambda_2} \int_0^{2\pi} \int_0^{\pi_2} L_s(\theta_i,\Phi_i,\lambda_i)\mathrm{Sin}\theta_i\mathrm{Cos}\theta_i d\theta_i d\Phi_i d\lambda_i. \tag{3}$$

Likewise, the total power reflected from the surface element may be described by

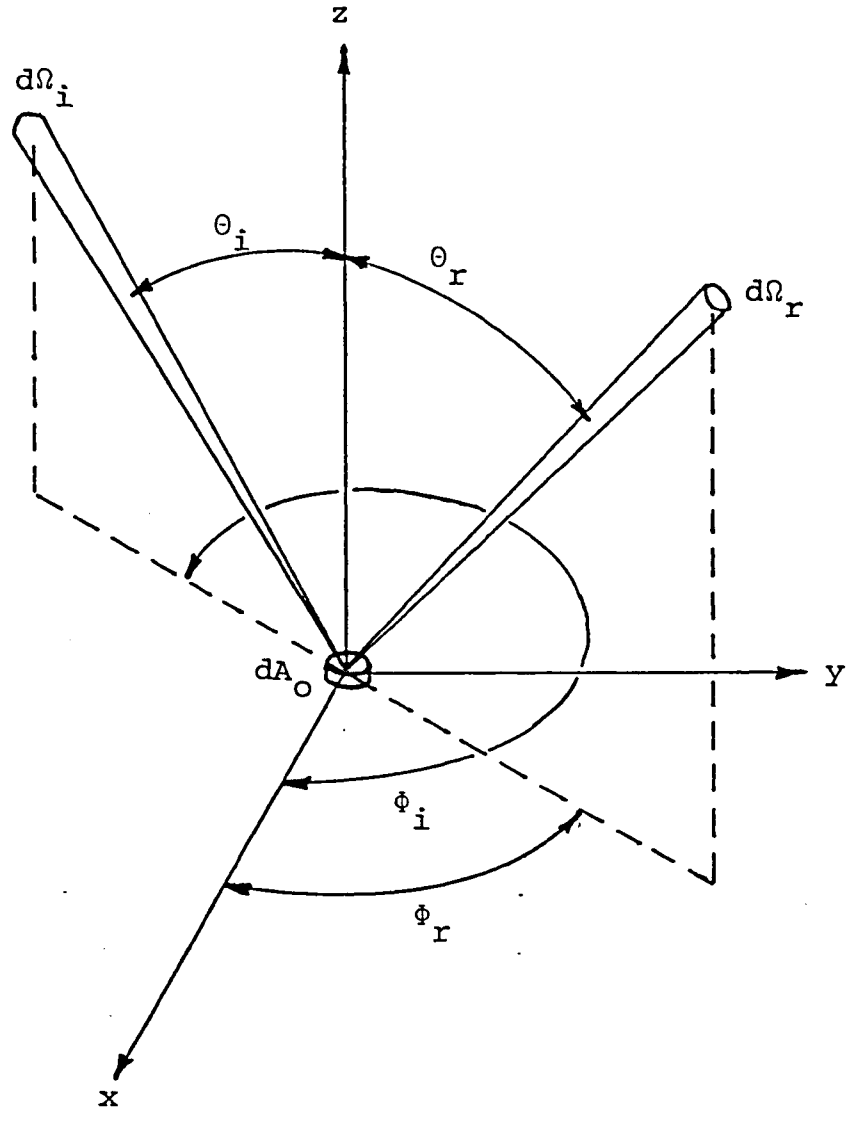

Figure 1. Reflectance geometry -- The geometry used in describing the total reflectance.

$$P_r = \int_{\lambda_1}^{\lambda_2} \int_0^{2\pi} \int_0^{\pi_2} L_o(\Theta_r,\Phi_r,\lambda_r)\,\mathrm{Sin}\Theta_r\mathrm{Cos}\Theta_r\,d\Theta_r\,d\Phi_r\,d\lambda_r, \qquad (4)$$

where $L_o(\Theta_r,\Phi_r,\lambda_r)$ is the reflected radiance.

We can describe the reflected radiance $L_o(\Theta_r,\Phi_r,\lambda_r)$ as

$$L_o(\Theta_r,\Phi_r,\lambda_r) = R(\Theta_i,\Phi_i,\lambda_i)L_s(\Theta_i,\Phi_i,\lambda_i), \qquad (5)$$

where $R(\Theta_i,\Phi_i,\lambda_i)$ is the reflectance function of the surface. The total (hemispheric) reflectance of the surface may then be expressed by

$$R_t = \frac{\int_{\lambda_1}^{\lambda_2} \int_0^{2\pi} \int_0^{\pi_2} R(\Theta_i,\Phi_i,\lambda_i)L_s(\Theta_i,\Phi_i,\lambda_i)\,\mathrm{Sin}\Theta_i\mathrm{Cos}\Theta_i\,d\Theta_i\,d\Phi_i\,d\lambda_r}{\int_{\lambda_1}^{\lambda_2} \int_0^{2\pi} \int_0^{\pi_2} L_s(\Theta_i,\Phi_i,\lambda_i)\,\mathrm{Sin}\Theta_i\mathrm{Cos}\Theta_i\,d\Theta_i\,d\Phi_i\,d\lambda_i}. \qquad (6)$$

In the case of reflections from optically rough surfaces such as those of most building materials, the diffuse approximation suggested by Duffie and Beckman (1974, p. 94) can typically be applied. That is, the reflectance is assumed to be independent of direction, Θ and Φ. Also, the incident and reflected bandwidths are assumed to be the same, $\lambda_i = \lambda_r$. With $\Theta_i = \Theta_r$ and $\Phi_i = \Phi_r$, we see all that remains to obtain the total reflectance is to measure both the reflected radiant power and the incident radiant power and take the ratio between them.

Lambertian Response

A color compensated probe with a diffuse Lambertian response receiving element was employed to measure the total radiant power described above. Referring to the geometry in Figure 2, we can examine the properties of a Lambertian response in more detail.

If the source dA_1 has a radiance $L(\Theta,\Phi)$ $\frac{\text{watts}}{m^2 s}$, then the differential power dP on dA_2 may be described as

$$dP = L(\Theta,\Phi) \frac{dA_1}{R^2} \text{Cos}\Theta dA_2. \tag{7}$$

Note that the term $\frac{dA_1}{R^2}$ CosΘ describes the solid angle subtended by dA_1 onto dA_2. As dA_2 may be expressed by

$$dA_2 = R^2 \text{Sin}\Theta d\Theta d\Phi, \tag{8}$$

dP may also be written as

$$dP = L(\Theta,\Phi) dA_1 \text{Cos}\Theta \text{Sin}\Theta d\Theta d\phi. \tag{9}$$

To obtain the total hemispherical power P_h, we simply integrate and get

$$P_h = \int_0^{2\pi} \int_0^{\pi/2} L(\Theta,\Phi)\, dA_1\, \text{Cos}\Theta \text{Sin}\Theta d\Theta d\Phi. \tag{10}$$

If the source is Lambertian, which means that the radiance is constant and independent of direction, and dA_1 being representative of a small element of area A, we can describe the radiant exitance M, as

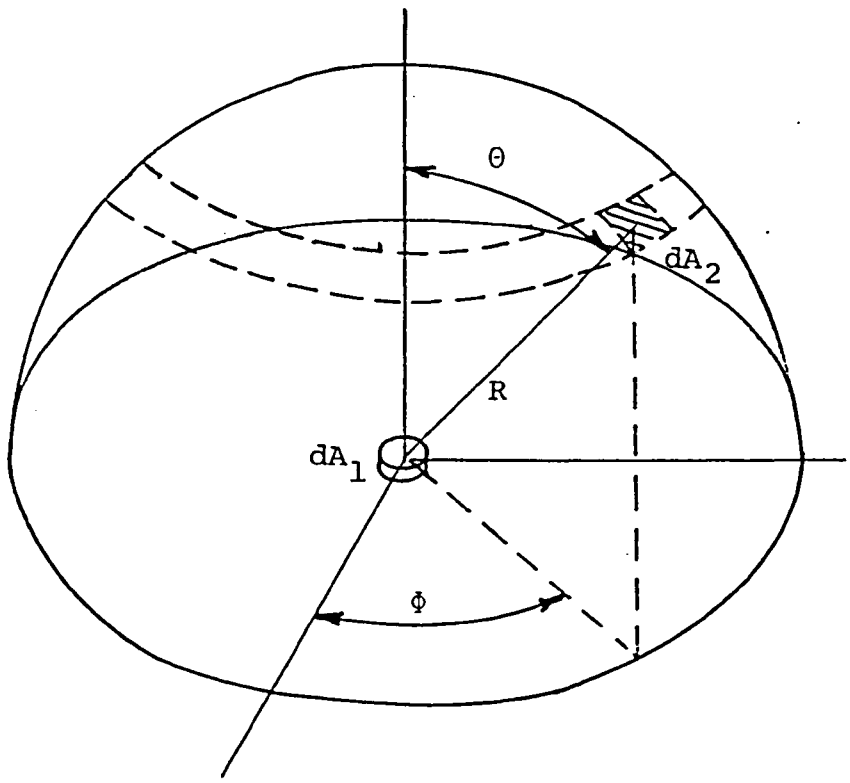

Figure 2. Radiation geometry -- The geometry used in describing a Lambertian response.

$$M = \frac{P_h}{M} = \pi L \frac{\text{watts}}{m^2}. \tag{11}$$

Thus, the Lambertian source radiates power per unit source area into 2π steradian, which is π times the source radiance. Now if we let dA_1 be called the receiving element, we can invoke reciprocity and state that the Lambertian receiver collects the irradiance from 2π steradians. Since each element of irradiance or incident flux is adjusted by the cosine of the angle from the surface normal and the receiving element is assumed diffuse and isotropic, the response of the probe is independent of elevation and azimuth. Also, with the probe being color compensated, its response is independent of the input wavelength.

INSTRUMENTATION

The instrumentation utilized in this study was developed during an undergraduate senior project undertaken by L. R. Anderson and this author in 1975. The system consisted of an optical probe and a digital control and display unit. The optical probe incorporated a diffuse receiving element that was designed by Huttenhow (1976) as part of his Master's thesis work at The University of Arizona. This receiving element has essentially a Lambertian response. That is, an incident ray of radiant flux is appropriately weighed by the cosine of the incident angle from the surface normal. Also, the probe uses a color compensated photodiode that makes its response essentially independent of wavelength.

The mechanics of the optical probe (Figure 3) consists basically of a color corrected photodiode mounted behind the diffuse receiver. The main housing was machined from aluminum and was designed to mount on a standard camera tripod. Two sets of pinhole sights (Figure 4) along with an added protracter scale on the tripod allowed for direct sun alignment of the probe and the determination of the sun elevation angle. A light pipe was used to transmit the collected radiant flux from the receiving element back through the baffled and flat black painted interior of the

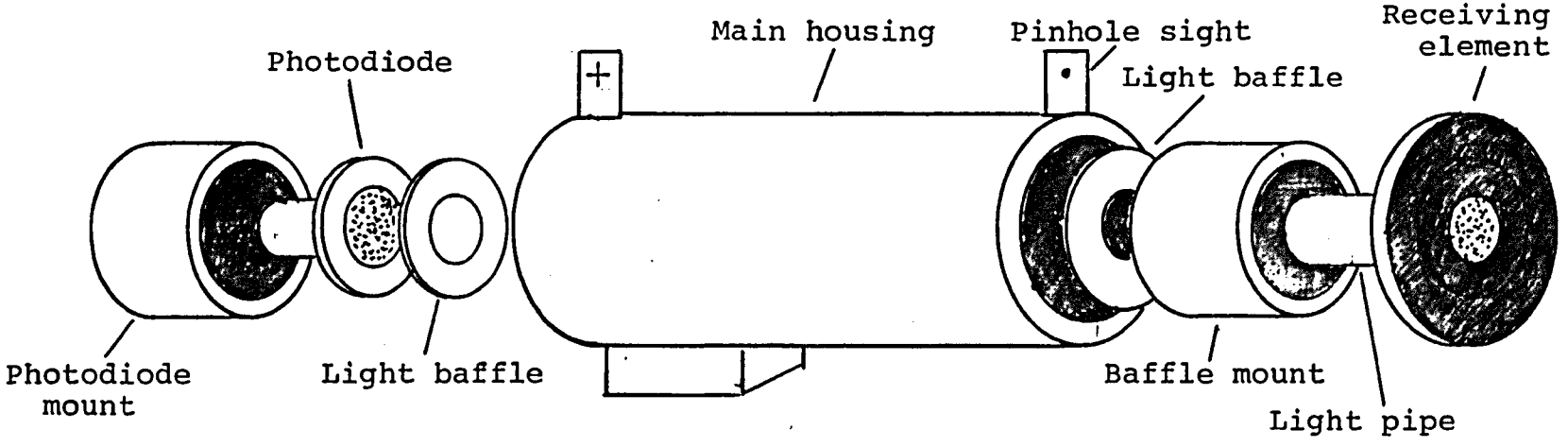

Figure 3. Optical probe assembly.

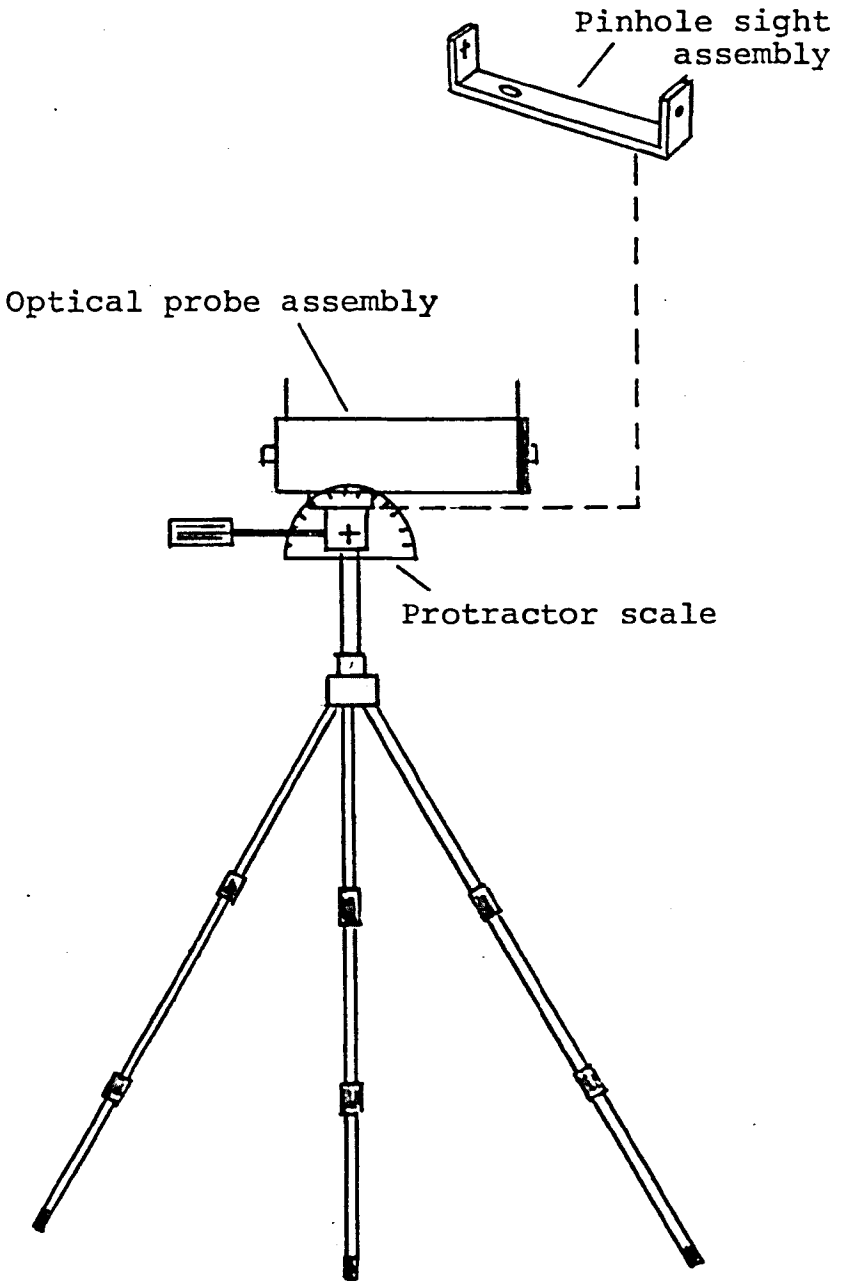

Figure 4. Tripod mount assembly.

main housing to the photodiode. The photodiode utilized in the probe was a United Detector Technology Inc. PIN-10DF having a response (Figure 5) that is essentially flat over the 0.45 to 0.95 μm bandwidth. Even though this does not cover the entire solar energy spectrum (Figure 6) the probe does respond to most of the total radiant energy within this spectrum. In addition, other sources of reflectance values such as Kreith (1973, pp. 238-239) show that the reflectance values for materials typically found in building materials do not change significantly in the remaining 0.95 to 2.5 μm portion of the spectrum.

The diode was biased in the photovoltaic mode (Figure 7) such that the output, displayed at the radiometer Control and Display Unit, was a voltage proportional to the incident power. The Control and Display Unit contained the photovoltaic circuitry as well as the digital voltmeter circuitry.

Since the optical system collected total radiant flux, which includes the direct solar, diffuse solar, and background radiant fluxes, an occulting disc was fashioned such that it could be held in front of the receiver so as to block the direct component and enable the measurement of the combined diffuse and background radiation term. An "A-Frame" type unit (Figure 8) was fabricated to mount the optical probe assembly for horizontal and sloped surface measurements. The probe could be rotated about the center

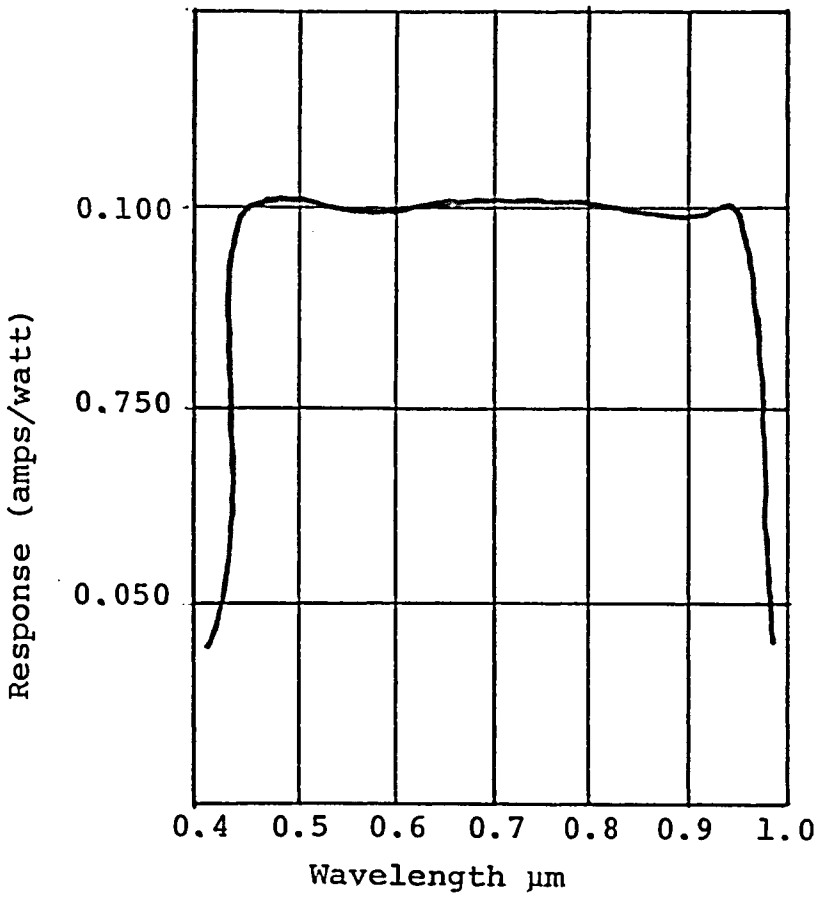

Figure 5. Photodiode response curve -- Typical response of a United Detector Technology Inc. PIN-10DF detector/filter combination.

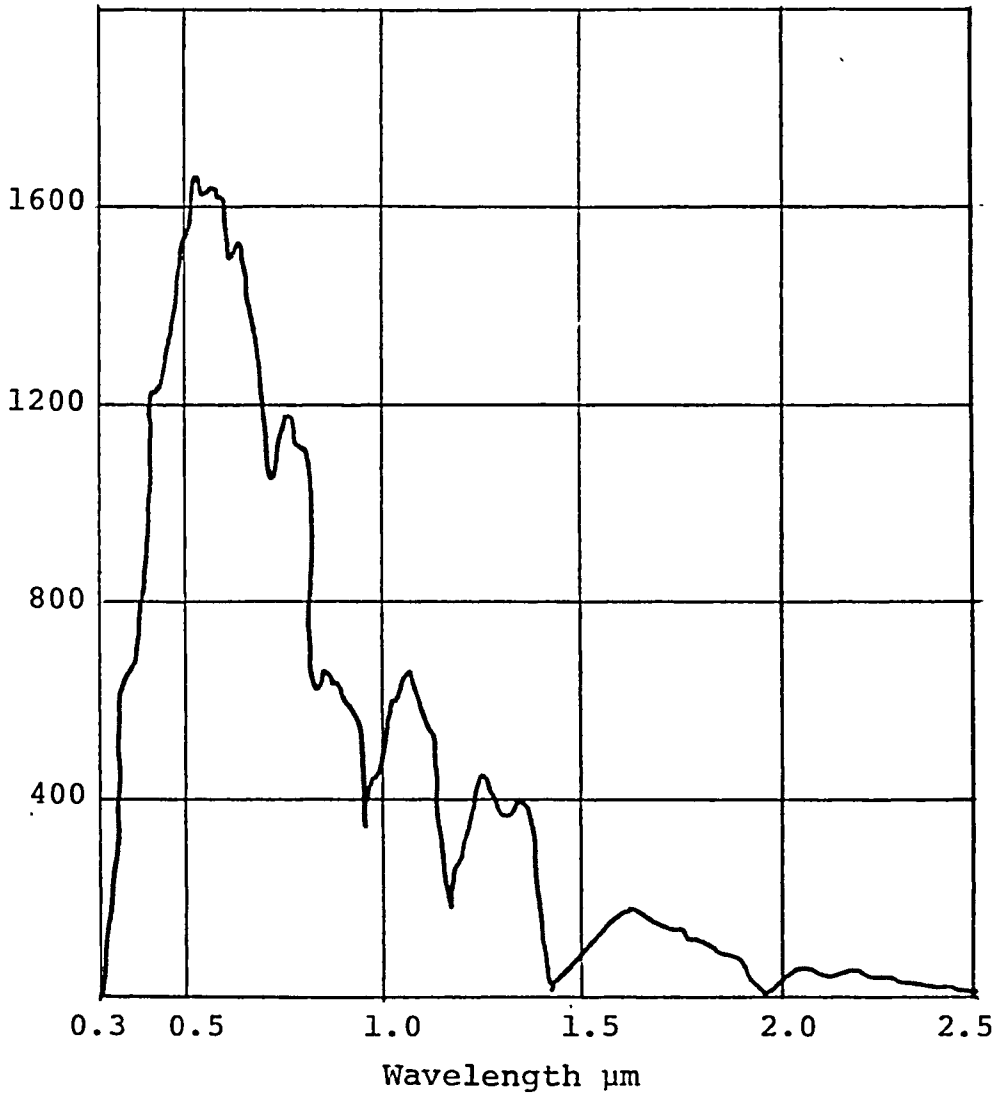

Figure 6. Solar spectral intensity curve -- Solar energy spectrum for airmass on and molecular absorption (Duffie and Beckman, 1974, p. 14).

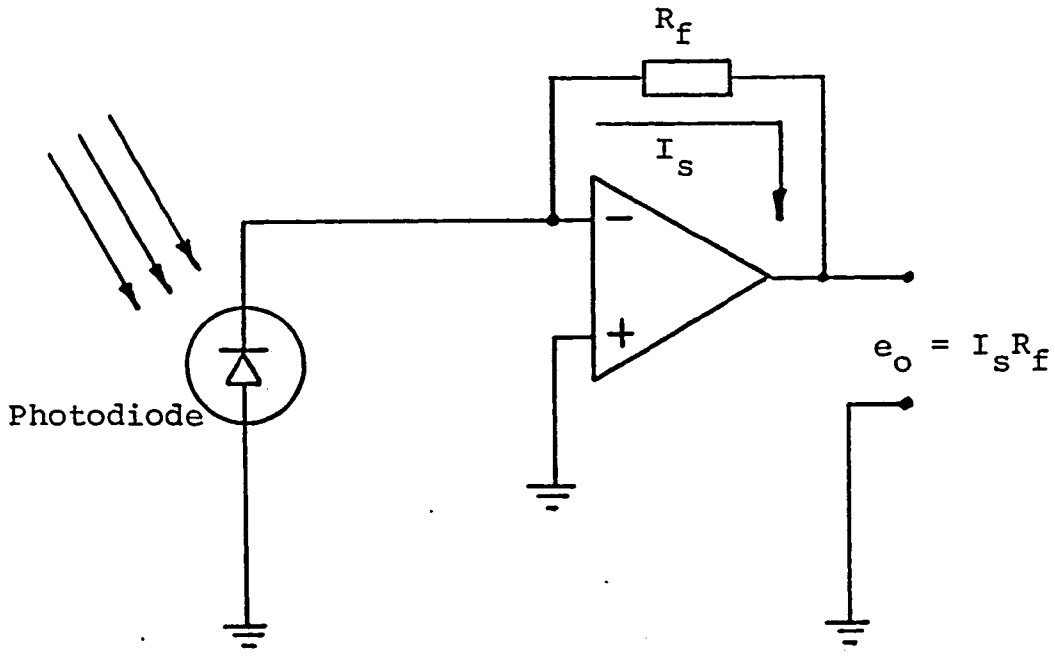

Figure 7. Photovoltaic circuit -- Photodiode connected in the photovoltaic mode of operation using an operational amplifier.

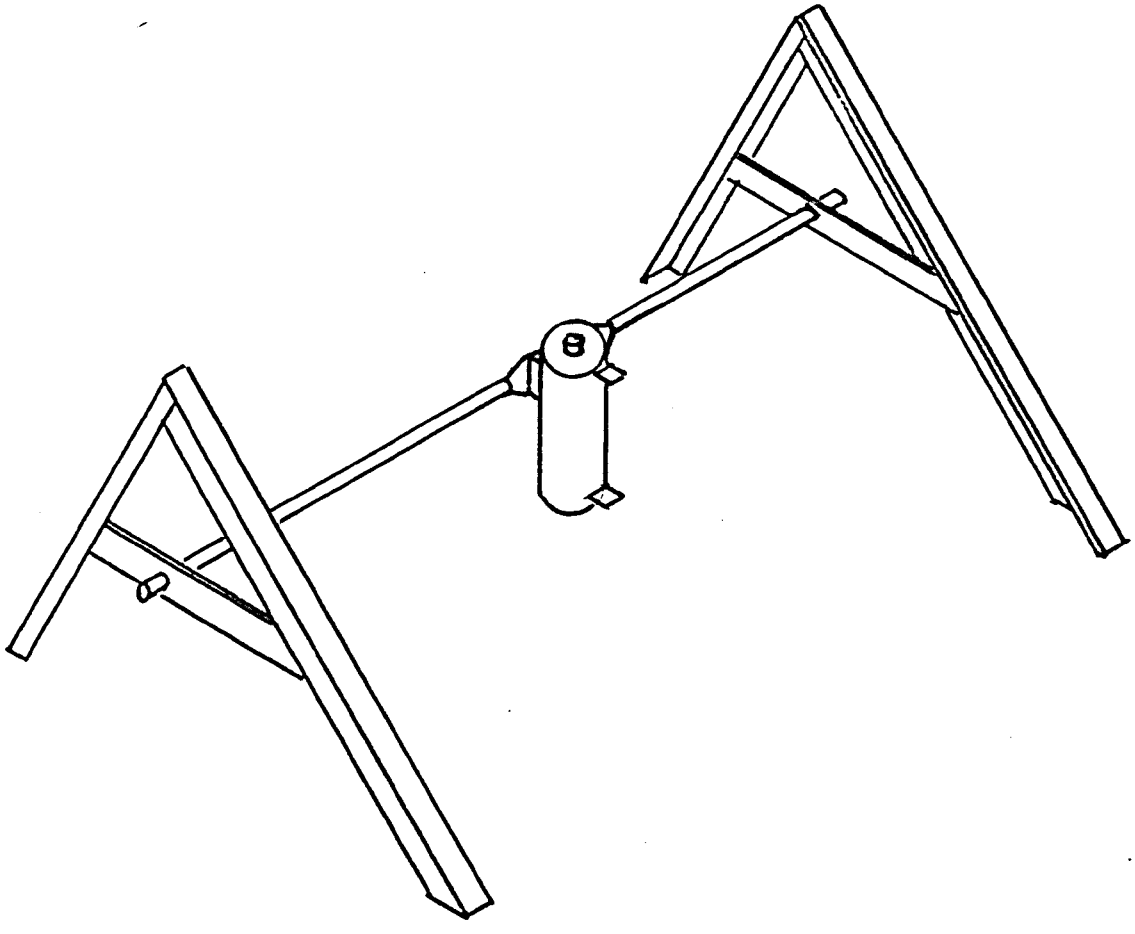

Figure 8. "A-Frame" mount assembly.

line axis and locked in any angular position. The incident sun angle measurements were realized using the tripod and pinhole sight assembly as detailed in the measurement procedures section of this thesis.

EXPERIMENTATION

Optical Probe Lambertian Response Verification Experiment

An experiment was conducted to verify that the optical probe had an acceptable Lambertian response. An occulting ball was fashioned such that it could be positioned in front of the diffuse receiving element. The ball subtended a shadow onto this element, that was approximately a half of a degree larger than the element itself. This was accomplished using

$$W' = W + \pi/360\ R, \tag{12}$$

where W' is the diameter of the occulting ball, W is the diameter of the diffuse receiving element, and R is the distance between them. This occulting ball made it possible to determine the direct component of the incident radiant flux. This was accomplished by simply subtracting the occulted reading from the unocculted reading.

If the probe's response was nearly Lambertian, then the ratio of the normal to horizontal direct components would have to be equal to the cosine of the incident sun angle. Measurements were made over a large range of incident sun angles and the results (Table 1) show that the probe did have a response which was very close to being perfectly Lambertian.

Table 1. Lambertian response verification experiment data.

Incident sun angle	Cosine of sun angle	Ratio of normal to horizontal
24	0.9135	0.9102
25	0.9063	0.9048
26	0.8988	0.8988
29	0.8745	0.8698
32	0.8480	0.8383
37	0.7986	0.8025
39	0.7771	0.7791
43	0.7314	0.7222
46	0.6947	0.7070
49	0.6561	0.6471
52	0.6157	0.6194
55	0.4736	0.5724
61	0.4848	0.4722
67	0.3907	0.3846
76	0.2419	0.2404
81	0.1564	0.1395
84	0.1045	0.0952
89	0.0175	0.0103

Optical Probe Target Size Response Experiment

This experiment was undertaken to examine the optical probes response to a specific change in target size. Since the probe senses total radiant flux, it actually sees more than just the surface we are measuring. However, with the probe placed near the surface, the reflected flux collected by the probe should be essentially that reflected from the surface we are interested in.

Physical limitations on the probe and tripod assembly dictated a six inch probe to surface separation. Wall and roof structures generally are large enough such

that at this distance they will subtend almost a full 90 degree solid angle. This is probably a better assumption for a roof than a wall because walls are generally obstructed with overhangs, windows, and surrounding vegetation. Thus we are usually confined to about a four to six foot diameter circular target area for the wall measurements.

Theoretically, the four foot diameter target would subtend a 75 degree solid angle and a six foot diameter target would subtend an 81 degree solid angle at the six inch probe separation. We can determine the total reflectance from Equation (6) which yields

$$R_t = R_1 \, \mathrm{Sin}^2 \, \theta \Big|_0^a + R_2 \, \mathrm{Sin}^2 \, \theta \Big|_a^{90°}, \qquad (13)$$

where the diffuse approximation has been made to bring the terms R_1 and R_2 outside the integrals. The term R_1 is the target reflectance and R_2 is the reflectance outside the target area. From this we find that a six foot diameter target would contribute 97 percent of the total reflectance value, a four foot diameter target would contribute 93 percent. It is my contention that the remaining three to seven percent of the total reflectance value, the R_2 term, will contain enough of the desired surface reflectance value as long as the target area is selected appropriately.

That is, there should be a minimum of sharp contrasts, obstructions and shadows in and just outside the target area.

To examine the probe's response to a change in target size, a six by seven foot plywood target was constructed. The target was positioned in a good solar exposure. Four reflectance values were measured using the tripod mounted probe at a six inch separation. These were first the plywood, then a six foot target area, then a four foot target area, both of which were plain plywood masked off using black paint, and last the entire target painted black. Theoretically, the six foot target total reflectance, call it R_6, is made up of

$$R_6 = R_2 \, \mathrm{Sin}^2 \, \theta \Big|_0^{81^\circ} + R_o, \tag{14}$$

where R_2 is the reflectance of the plywood and R_o is the reflectance value of the mask and background residuals. By subtracting the measured value of R_6 from the measured value of R_w we are left with a value for R_o.

For the four foot diameter target the total reflectance value, R_4, is made up of

$$R_4 = R_w \, \mathrm{Sin}^2 \, \theta \Big|_0^{75} + R_p \, \mathrm{Sin}^2 \, \theta \Big|_{75}^{81} + R_o, \tag{15}$$

where R_p is the measured value of reflectance of the black paint. From Equations (14) and (15) and the measured

values of R_6, R_o, and R_p, we can then predict that R_4 will be

$$R_4 = (R_6 - R_o)0.9564 + (R_p)0.0425 + R_o. \quad (16)$$

The results of this experiment (Table 2) show that the probe was able to predictably detect the change of reflectance value for this change in target size. However, these values are small even though the target size was reduced using a sharply contrasting mask. Thus we see that the probe will yield a representative reflectance value for the surface being measured.

Table 2. Optical probe response to a target size change.

Measured values					Predicted value
R_w	R_6	R_p	R_o	R_4	R_4
0.5813	0.5714	0.0579	0.0099	0.5555	0.5494

Optical Probe Azimuth and Elevation Independence Experiment

This experiment was conducted on the premise that the optical probe's Lambertian response was independent of the incident sun angle. The desired result of this experiment should show that the instrumentation can obtain

essentially the same reflectance value for a surface regardless of the incident sun angle.

A six foot diameter target, painted white, was constructed. The target was first positioned vertically and in a western solar exposure. Reflectance measurements were made at fifteen minute intervals over a four hour period. The experiment was conducted again for an eastern and southern solar exposure. Finally, the experiment was conducted for a horizontal target position. The results of these observations are shown in Figure 9. The reflectance values measured in this experiment show that the probe is essentially independent of the azimuth and elevation incident sun angle. Also it should be noted that the results demonstrate that the reflectance of the surface itself follows the diffuse approximation by remaining constant over this angular range for which the measurements were made.

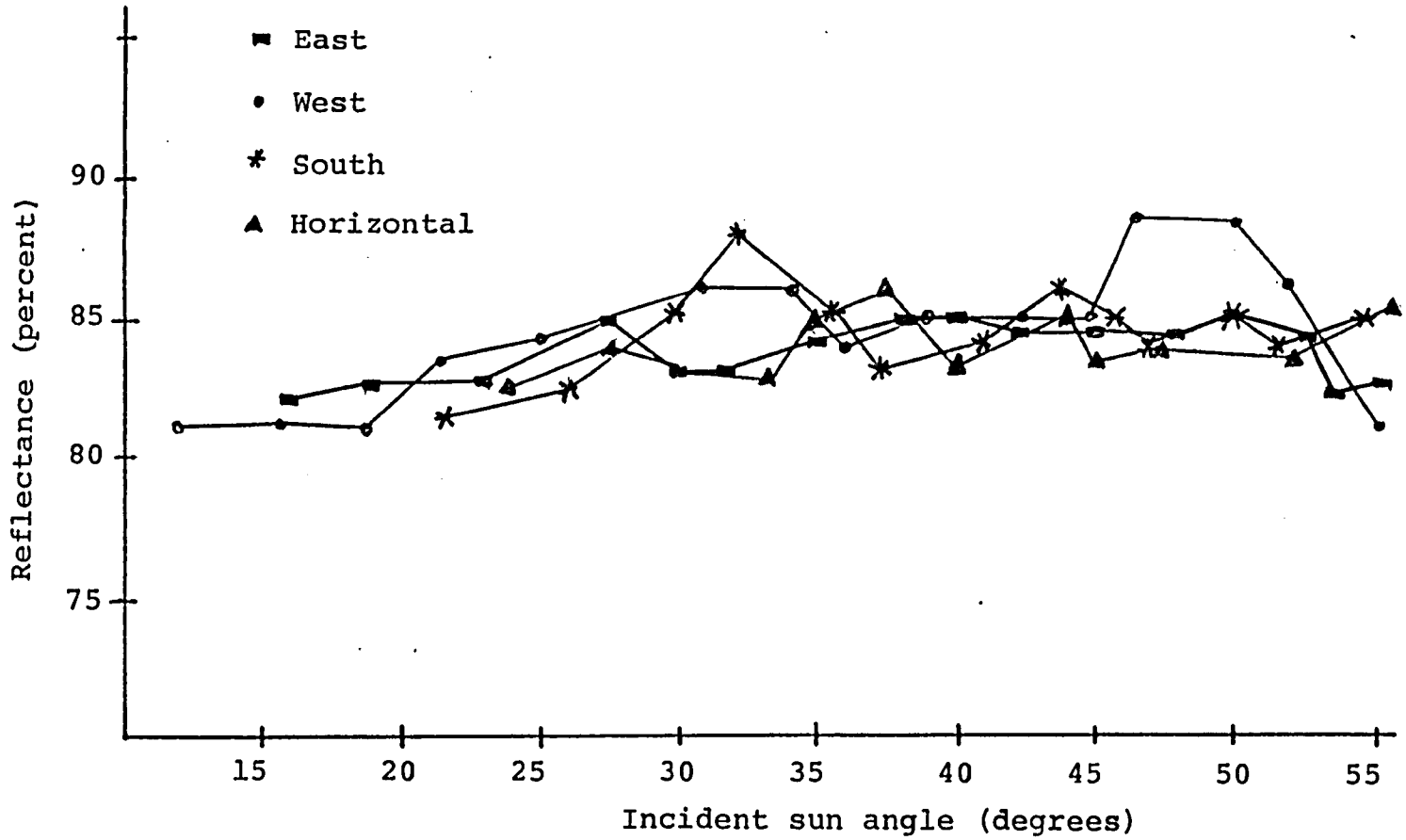

Figure 9. Reflectance plot -- Reflectance of a six foot diameter test target for east, west, south, and horizontal exposures and over varying incident sun angles.

MEASUREMENT PROCEDURES

Vertical Surface Measurement

This type of measurement proved to be the most difficult. The major difficulty was that of finding a target surface area with good solar exposure which was not obstructed by surrounding vegetation. Generally, this could be realized only at certain times of the day when that particular target area would have the proper exposure. Consequently, it was not possible to measure all surfaces of interest.

What constituted a target surface area was that region of an unobstructed portion of wall in which a circle of diameter of approximately four to six feet, could be inscribed. Depending on the specific surface texture the target area should have a minimum of self shadowing, a factor that could be obtained by avoiding high direct sun angles. The surfaces were selected so that a minimum of two such target areas were available so that an average reflection value could be obtained.

After the surface was located it was then documented on a data sheet as to its type of structure, material, color, and exposure, along with its location, cloud condition, and compass orientation. With the surface identified, the optical probe was then set up. The probe was

mounted on the tripod and then adjusted and leveled using a bubble level so that the receiving element was aimed at the target area center and was six inches away from the surface. This alignment constituted the reflected measurement position. Next, the optical probe was rotated 180 degrees and leveled again. This left the probe looking directly away and normal to the target area center which defined the appropriate orientation to measure the incident flux. By using an occulting disc to block out the direct sun, the diffuse component of the incident flux could be measured. Next, by utilizing the pinhole sight system on the optical probe housing, the unit was positioned in azimuth and elevation so that it was aimed directly at the sun for the direct sun measurement. By adjusting the probe in elevation only to the leveled horizontal position and setting the protractor scale on the tripod to the zero reference position, the direct sun elevation angle could be measured upon reacquisition of the direct sun measurement position.

Horizontal and Sloped Surface Measurements

This type of measurement differed slightly from the vertical surface type measurement. The "A-Frame" optical probe mount could be used only for measuring the incident, diffuse, and reflected flux values. The absence of an azimuth adjustment on this unit prevented the making of

the direct sun measurement. Sloped surface observations were also limited to an "eye-ball" type of alignment for both the incident total and reflected positions due to the unusability of a bubble level in this type of observation. However, after a little practice on a horizontal surface and with the aid of an alignment mark on the "A-Frame" center line shaft, this type of measurement was made with essentially no variation from that of a bubble leveled type of measurement.

The direct sun angle was determined by utilizing the tripod assembly with a pinhole sight bracket mounted in place of the optical probe. In the case of a sloped surface, the complete tripod and sight had to be leveled, using a bubble level, on a level surface. The protracted scale was then adjusted to the zero position. With the "A-Frame" mounted optical probe assembly positioned on the sloped target surface, the pinhole sight and tripod assembly was positioned at the target area in azimuth with the incident direct sun. By adjusting the pinhole sight in elevation to the direct sun alignment position, the direct sun angle, in elevation from the target surface normal, could be measured.

The total reflectance value was obtained by simply taking the ratio of the reflected measurement voltmeter reading to that of the incident measurement voltmeter reading. Since exterior walls and roofs are quite

heterogeneous and anisotropic in the general sense, averaging of the measurements was made to minimize these effects.

RESULTS AND DISCUSSION

The intent of this thesis was to measure solar reflectance values associated with building materials. Sixty-eight different building material surfaces and six miscellaneous ground surfaces were measured and cataloged. All of these observations are cataloged in Tables 3 through 9.

The reflection values obtained were found to be in general agreement to what was expected. That is, surfaces which appeared to be light, medium, or dark in color generally yielded, when measured, comparable reflectance values. Also, surfaces that had rough textures were typically found to have lower reflectance values than comparably colored surfaces with smooth textures. This was most likely due to the rough texture trapping more of the incident radiant flux thus allowing less of the radiant flux to be reflected.

There were two measurements that were found to be exceptions to what was expected. The Avocado Green paint (Table 6) appeared to be a medium color. However, when measured it was found to be quite dark. This was a case where the photopic response of the human eye was deceived. Another exception was for an asphalt shingled roof colored Snow White (Table 7). Again the surface appeared to be

Table 3. Walls, block construction.

Description	Reflectance value
Burnt adobe block, running bond, tooled light grey mortar joint	36%
Same with raked joint	34%
Colored slump block, running bond, concave low contrast mortar joint	
Tan (San Xavier SX-15)	43%
Plain (San Xavier SX-16)	44%
Buff (Columbia Block)	39%
Santa Rosa (Columbia Block)	36%
Palo Verde (San Xavier SX-17)	33%
Coral San Xavier (SX-14)	38%
Adobe Red (Columbia Block) with raked joint	21%
Colored CMU (concrete masonry unit) running bond, concave low contrast mortar joint	
Coral (San Xavier SX-14)	34%
Adobe Red (San Xavier SX-26)	32%
Buff (Columbia Block)	31%
Plain or grey	39%
Same with plain joint	45%

Table 4. Walls, brick construction

Description	Reflectance value
Brown (PBY[a] color #19) scratch brick, common bond, concave medium grey mortar joint	28%
Same color ruffled brick, basket weave bond, same color and type joint	36%
Same with herringbone bond	33%
Light red (PBY color #16) scratch brick, common bond, concave medium grey mortar joint	38%
Orange (PBY color #06) ruffled brick, plain medium grey mortar joint	41%
Buff (PBY color #94) plain brick, stack bond stretchers, raked medium grey mortar joint	51%
Same color ruffled brick, English cross bond, concave medium grey mortar joint	43%
Same color scratch brick, running bond, plain medium grey mortar joint	41%
Red (PBY color #04) ruffled brick, third bond oversize brick, raked medium grey mortar joint	35%
Same color and type brick, English cross bond, concave medium grey mortar joint	34%

[a]Phoenix Brick Yard/Tucson Division color index.

Table 5. Walls, painted, block construction.

Description	Reflectance value
Painted slump block, running bond, concave joint	
Pearl White (Pioneer Paints)	74%
Navaho White (Pioneer Paints)	70%
White (Pioneer Paints)	71%
Spanish White (Pioneer Paints)	68%
Egg Shell White (Pioneer Paints)	65%
Mortar washed, solid grey coverage on slump block, same bond and joint	49%
Painted CMU (concrete masonry unit), same bond and joint	
Bone White (Southwestern Paints)	73%
Navaho White (Pioneer Paints)	72%
Sea Sheel Beige (Pioneer Paints)	55%
Pearl White (Pioneer Paints)	69%
Desert Sand (Sears)	42%

Table 6. Walls, painted or stained surfaces.

Description	Reflectance value
Painted stucco, Bone White (Southwestern Paints)	65%
Painted wood paneling	
Avocado Green (Pioneer Paints)	15%
Sand Dune (Pioneer Paints)	26%
Beige (brand unknown)	40%
Stained wood paneling	
Weathered Brown (2310 Southwestern's wood stain)	10%
Dark Brown (2302 Southwestern's wood stain)	13%

Table 7. Roofs, shingled

Description	Reflectance value
Asphalt tab shingles, common lay	
Woodblend (GAF)	17%
Russet Blend (GAF)	9%
Autumn (Flintkote)	10%
Frosted Red (Flintkote)	20%
Canyon Red (Flintkote)	13%
Snow White (Flintkote)	24%
Dark Mahogany (GAF)	8%
Pastel Green (GAF)	16%
Earthtone Brown (GAF)	9%
Blizzard (Fire King)	34%
White (JM)	33%
Red (JM)	14%
Clover Green (Flintkote)	11%
Shake cedar wood shingles, new, unoiled	32%
Same but oiled	28%
Red clay mission tile	26%

Table 8. Roofs, built up construction.

Description	Reflectance value
Pea gravel covered	
Dark blend	12%
Medium blend	24%
Light blend	34%
Crushed used brick, red, covered	34%
White marble chips covered	49%
Flexstone or mineral chip roll type, white	26%
Polyurethane foam, white coated	70%
Same with tan coating	41%
Silver, aluminum painted tar paper	51%
White coated, smooth, Kool Kote (Corbett Roofing Co.)	75%
Tarpaper, "bleach out"	41%

Table 9. Miscellaneous, ground surfaces.

Description	Reflectance value
Grass, mowed	25%
Desert soil, natural	29%
Weathered asphalt driveway	19%
Redwood decorative chips, weathered	19%
Concrete slab, smooth, light grey	36%
Crushed used brick, red, decorative landscape	30%

a light color but when measured it was found to be rather dark. However, after a closer examination of the shingles, the reason for the low value of reflectance became more obvious. The coverage of the white mineral particles on the shingles was found to be rather thin and thus exposed a good portion of the asphalt base. Also, the edges of the shingles were very dark. Thus this particular roof was really more a grey color than white.

Brand names were used only to aid in the identification of the surface being measured. By no means was an attempt made to rate the quality of these products. For an example, there are an almost uncountable number of paint manufacturers that produce house paint in the color off white. Each one, although having the same color name, can differ slightly in shade. In addition, the ocular appearance alone does not determine the reflectance value of the paint. The constituants of the paint and even the surface that it is applied to also affect the reflectance value. Thus, by using these brand names, we are simply able to better identify the surface reflectance value obtained.

These reflectance values presented here should be of value in the determination of the heating/cooling loads of structures common to the Southwest by providing information that has not been readily available in the past. The total reflectance value is particularly important in

characterizing the solar contribution to the net transfer of heat through a sunlit opaque building element. This can be seen by the fact that the total reflectance value R_t, for an opaque surface is related to the absorbance value α, by

$$\alpha = 1 - R_t. \tag{17}$$

This absorbance value must be known in order to calculate the heat flow into a sunlit surface. From the ASHRAE Handbook of Fundamentals (1972, p. 410), we see that the heat flux q, per unit area A, into a surface is

$$q/A = \alpha I_t + h_o(t_o - t_s) - \varepsilon \Delta R. \tag{18}$$

The term I_t is the total solar radiation incident on the surface. The term h_o is the coefficient of heat transfer for the surface air film, typically a value of 3 to 4. The $(t_0 - t_s)$ term is the difference between the outside air temperature and the surface termperature. The $\varepsilon \Delta R$ term is made up of ε, the hemispherical emittance value of the surface, and ΔR which is the difference between the long-wave radiation incident on the surface and that which would be emitted from a black body at this surface temperature. A typical value for $\varepsilon \Delta R$ is about 20 BTU/HrFt^2. From absorbance values inferred from these measurements of reflectance, it is evident that the absorbance value of the surface is a major factor in this heat flow calculation.

In addition to the reflectance values obtained from these observations, these data yielded two other values related to the cooling load calculations. In the ASHRAE Handbook of Fundamentals (1972), the diffuse solar radiation factor, C, is tabulated for the 21st day of each month. This factor can be expressed as the ratio of the diffuse solar radiation, I_{ds}, for a clear sky, to the direct normal solar radiation, I_{DN}. It can also be related to the total horizontal radiation, I_{th}, as

$$C = (I_{th}/I_{DN}) - \text{Sin } \beta, \tag{19}$$

where β is the sun elevation angle from horizontal.

During the month of June, several observations were made of horizontal surfaces. Data from these observations were used to compute values of C. Since the "A" frame probe mount did not allow for a direct sun measurement, the I_{DN} term also had to be computed. This was accomplished using the values from the horizontal surface observations as indicated,

$$I_{DN} = \frac{\text{Incident total horizontal - diffuse horizontal}}{\text{Sin } \beta}. \tag{20}$$

The results of these calculations, along with the measured data are shown in Table 10. The calculated values of C are compared to the interpolated values of C from the ASHRAE Handbook of Fundamentals (1972) table. The computed

Table 10. Diffuse solar radiation factor data from observations made in June.

Date	β (degrees)	I_{th} (volts)	I_{ds} (volts)	I_{DN} (volts)	C	C*
14	58	2.08	0.17	2.25	0.08	0.131
14	79	2.22	0.16	2.10	0.08	0.131
15	71	2.16	0.16	2.10	0.07	0.131
15	81	2.06	0.16	1.92	0.09	0.131
15	78	2.04	0.17	1.91	0.09	0.131
18	60	1.99	0.21	2.06	0.09	0.133
20	61	1.99	0.27	1.97	0.14	0.134
24	47	1.56	0.22	1.86	0.11	0.134
28	72	2.10	0.16	2.04	0.08	0.134
28	61	1.77	0.15	1.85	0.08	0.134

*Interpolated from ASHRAE Handbood of Fundamentals (1972) value.

Note: I_{th}, I_{ds}, and I_{DN} are in relative units of volts proportional to the sensed flux values.

values are slightly lower but of the same order of magnitude as the tabulated values. This I suspect can be attributed somewhat to the method I used to occult the sun for the diffuse measurement but mainly to the clearness of the Tucson sky. The Lambertian response verification experiment, accomplished in September, also yielded some data that this factor, C, could be computed from. In this experiment, the occulting device was constructed so that it would reliably occult the solar disc plus an additional half of a degree. All the values of I_{th}, I_{ds}, I_{DN} and β were measured, so that computed values for C could be

obtained from both the ratio of I_{ds} to I_{DN} and by Equation (20). The results of using the two methods for computing C are compared in Table 11. It can be seen that they are consistent and in close agreement. However, the interpolated value of C from the ASHRAE Handbook of Fundamentals (1972) is not in close agreement. This can be expected since only a single day's observation was used and the ASHRAE value is based on an average over many days.

The ASHRAE Handbook of Fundamentals (1972) also tabulates solar heat gain factors for the specific compass orientation at 32 degrees north latitude. Since the instrumentation used in this study was not an absolute measuring device, that is, it only indicated a proportional voltage value to the incident radiant flux collected by the receiver, this heat gain factor was not directly measurable. However, data were obtained that could be compared with the tabulated values by determining the ratios of the incident total measurements for the specific compass orientation to that of the computed I_{DN}. Data taken on the 23rd of June at 2:30 p.m. solar time were used to make this comparison with that interpolated data from the handbook. The results of this are presented in Table 12. Again it can be seen that these measured values are comparable to those of the handbook.

Table 11. Diffuse solar radiation factor data from September 5th observations.

β (degrees)	I_{th} (volts)	I_{ds} (volts)	I_{DN} (volts)	C	C*	Solar time
38	1.16	0.20	1.55	0.13	0.13	9:00 a.m.
44	1.36	0.25	1.57	0.17	0.16	9:35
51	1.52	0.25	1.63	0.16	0.15	10:05
58	1.66	0.26	1.67	0.15	0.16	10:35
61	1.73	0.26	1.69	0.15	0.15	11:05
64	1.80	0.29	1.68	0.17	0.17	11:35
66	1.83	0.31	1.67	0.18	0.19	12:05 p.m.
65	1.84	0.32	1.68	0.19	0.19	12:35
61	1.75	0.28	1.67	0.17	0.17	1:05
58	1.68	0.27	1.65	0.17	0.16	1:35
53	1.55	0.25	1.62	0.16	0.15	2:05
47	1.43	0.26	1.62	0.15	0.16	2:35
41	1.23	0.24	1.53	0.15	0.16	3:05
35	1.08	0.21	1.52	0.14	0.16	3:35
29	0.87	0.19	1.44	0.12	0.12	4:05
23	0.70	0.20	1.34	0.15	0.15	4:35
14	0.48	0.20	1.04	0.22	0.19	5:15
9	0.34	0.22	0.86	0.24	0.26	5:55

$C = (I_{th}/I_{DN}) - \text{Sin}$.

$C^* = I_{ds}/I_{DN}$

The interpolated value of C from the ASHRAE Handbook of Fundamentals (1972) is 0.107.

Note: I_{th}, I_{ds} and I_{DN} are in relative units of volts proportional to the sensed flux values.

Table 12. Solar heat gain factor data comparison for June 23, at 2:30 solar time.

	N	NW	W	SW	S	SE	E	NE	H
Calculated from ASHRAE Handbook data (1.15 SHG/ I_{DN})	0.15	0.47	0.72	0.56	0.17	0.15	0.15	0.15	0.95
Calculated from measured data ($\frac{\text{Incident total reading}}{\text{Computed } I_{DN} \text{ reading}}$)	0.08	0.23	0.48	0.48	0.24	0.09	0.09	0.09	0.62

SHG = Solar Heat Gain Factor (BTU/sq ft).

I_{DN} = Direct Normal Irradiation (BTU/sq ft).

Incident total reading (volts)

Computed I_{DN} reading (volts)

Note: The ASHRAE SHG factor must be multiplied by 1.15 to remove the effect of single pane 1/8" double-strength sheet glass.

SELECTED BIBLIOGRAPHY

Acklam, David M., and Lester R. Anderson. 1975. "Thermometer/Radiometer," EE203/299 Report, Dept. of Elec. Engr., Univ. of Arizona., Tucson.

ASHRAE Handbook of Fundamentals. 1972. Published by American Society of Heating, Refrigeration and Air-Conditioning Engineers, New York.

ASHRAE Standard 74-73. 1973. "Method of Measuring Solar-Optical Properties of Materials." Published by ASHRAE, New York.

Beckett, H. E. 1931. "The Reflecting Powers of Rough Surfaces at Solar Wave-Lengths," The Proceedings of the Physical Society, Vol. 43, Part 3, No. 238, pp. 227-241.

Cottony, Herman V., and Richard S. Dill. 1941. "Solar Heating of Various Surfaces," National Bureau of Standards Report, B.M.S. 64.

Duffie, John A., and William A. Beckman. 1974. Solar Energy Thermal Processes. New York: John Wiley & Sons, Inc.

Hechler, F. G., and E. R. Queer. 1933. "Surface Absorption of Heat from Solar Radiation," Refrigerating Engineer, Vol. 25, No. 2, pp. 86-91.

Heilman, R. H., and R. W. Ortmiller. 1950. "Effective Solar Absorption of Various Colored Paints," Trans. Am. Soc. Heat. Vent. Engrs., 50, pp. 399-410.

Huttenhow, Jay D. 1976. "Design and Analysis of a Spectrally Narrow-Band Radiometer." Master's thesis, Dept. of Elec. Engr., Univ. of Ariz., Tucson.

Kreith, Frank. 1973. Principles of Heat Transfer. New York: Educational Publishers, pp. 238-239.

Stimson, Allen. 1974. Photometry and Radiometry for Engineers. New York: John Wiley & Sons, Inc.

Wolfe, William L. 1965. Handbook of Military Infrared Technology. U. S. Government Printing Office, Washington, D. C.